GI3.00005
52nd APS DPP, 9 November 2010, Chicago

Formation of High-beta Plasma and Stable Confinement of Toroidal Electron Plasma in RT-1

H. Saitoh, RT-1 Experiment, University of Tokyo, Kashiwa, Chiba, JAPAN

RT-1: Magnetospheric plasma experiment

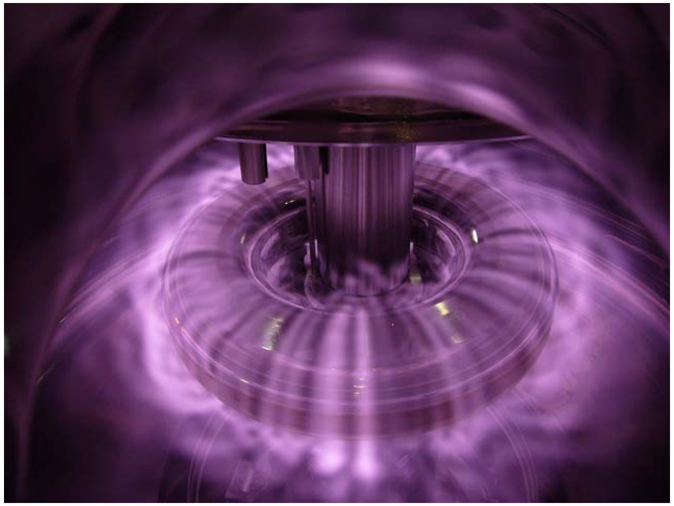

Magnetospheric plasma confined in RT-1

The RT-1 Experiment:
Z. Yoshida, Y. Ogawa, M. Furukawa, J. Morikawa, Y. Yano, Y. Kawai, H. Saitoh,
K. Harima, Y. Kawazura, Y. Kaneko, S. Emoto, M. Kobayashi, T. Sugiura, G. Vogel, H. Mikami, S. Iizuka

RT-1 Transdisciplinary Sciences, GSFS 東京大学 THE UNIVERSITY OF TOKYO

Levitated dipole system generates "Laboratory magnetosphere" with strongly inhomogeneous magnetic field

- RT-1: magnetospheric configuration generated by levitated dipole magnet*[1]

- Many interesting and fundamental properties of plasma can be investigated in its strongly inhomogeneous field

  - High-β plasma in Jupiter's magnetosphere
    - compressibility of flux tubes*[2]
    - effects of flow and dynamic pressure*[3]

  ➡ **Advanced fusion** using D-D and D-^{3}He

  - Inward diffusion and self-organization of stable vortex structures

  ➡ **Non-neutral plasma** including antimatters*[4]

  - Relation to Space plasma physics: Whistler waves, chorus emission, particle acceleration, substorms, etc.

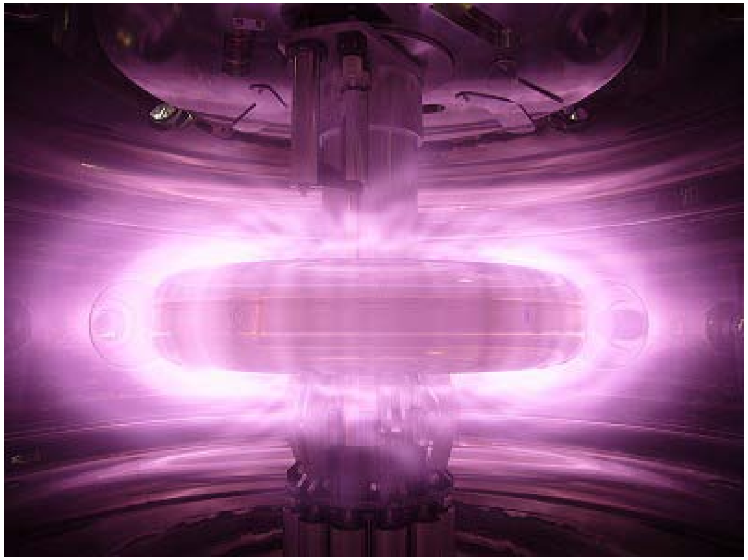

Magnetospheric plasma in RT-1

1. RT-1: 2010 Yoshida *et al*., PRL 104, 235004.
LDX: 2010 Boxer *et al*., Nat. Phys. 6, 207.

2. 1987 Hasegawa, CPPCF 11, 147.

3. 1998 Mahajan Yoshida, PRL 81, 4863;
2002 Yoshida Mahajan, PRL 88, 095001.

4. RT-1: 1999 Yoshida *et al*., in *NNP Phys. III*.
CNT: 2002 Pedersen Boozer, PRL 88, 205002.
LNT II: 2009 Stoneking *et al*., PoP 16, 0557708.

RT-1 has succeeded to generate high-β ECH plasma and to stably confine toroidal non-neutral (electron) plasma

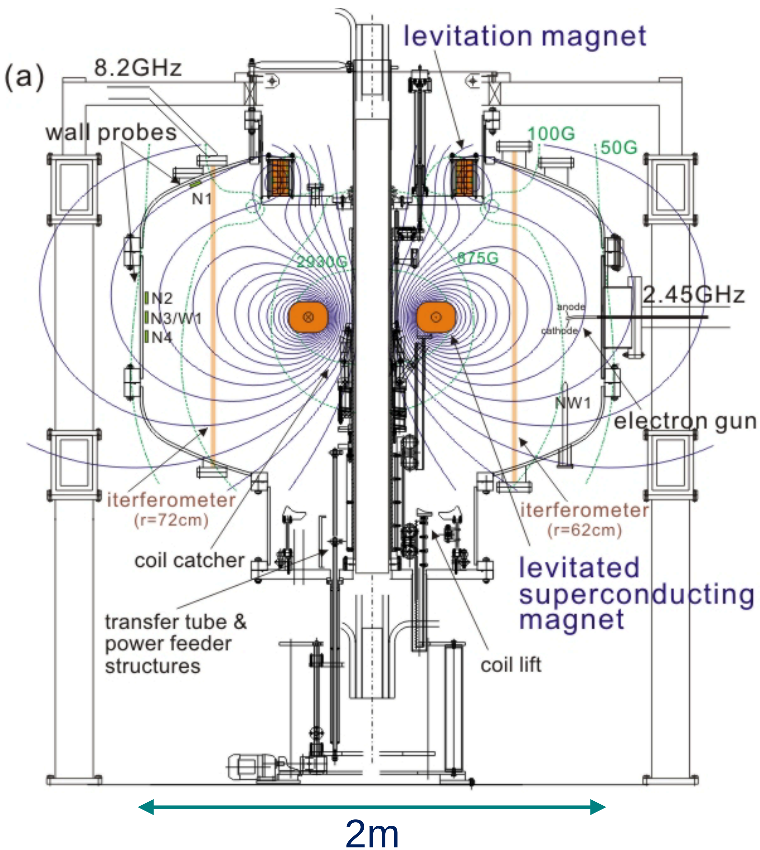

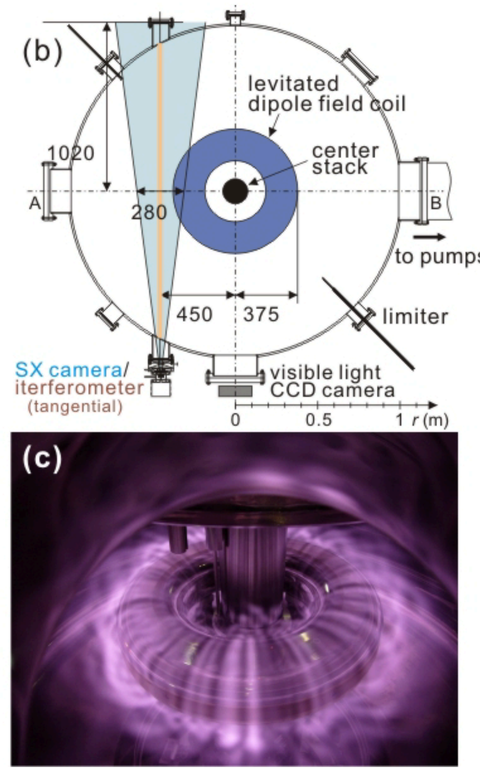

- HTS Bi-2223 magnet
  0.25MA,112kg
  magnetically levitated
- Microwaves
  8.2GHz (25kW) and
  2.45GHz (20kW)
- Electron gun
  LaB_6 cathode

Magnetospheric plasma Experiment, RT-1

2009 Ogawa *et al*., Plasma Fusion Res. 4, 020.

- **Toroidal non-neutral (pure electron) plasma**

  300s long confinement, rigid-rotating steady state, inward diffusion

- **High-β ECH plasma** *Yano et al*., Wednesday Morning NP9.39

  70% local β, confinement time ~0.5s, peaked density profile

Section I: Confinement of pure electron plasma

- Confinement time more than 300s for toroidal electron plasma
- Observations consistent with self-organization of rigid-rotating equilibrium
- Evidence for fluctuation induced radial transport through violation of third adiabatic invariants

2010 Yoshida *et al.*, PRL 104, 235004; 2010 Saitoh *et al.*, PoP in press.
2009 Saitoh *et al.*, Plasma Fusion Res. 4, 054.

Magnetospheric configuration enables stable confinement and novel studies of toroidal non-neutral plasmas*[1]

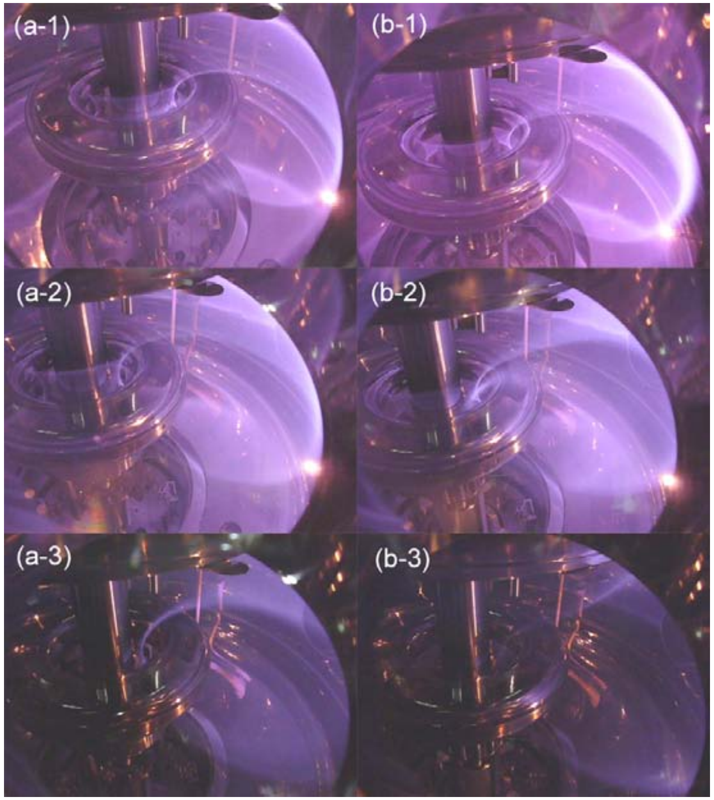

Visualized electron beam orbits agree with shape of magnetic surfaces.

- **Toroidal configuration can trap plasmas with arbitrary non-neutrarity**

  ➡ potentially applicable for antimatter plasmas

- **Magnetospheric toroidal NNP*[2]**

  - Axisymmetric trap: conservation of canonical angular momentum or 3rd adiabatic invariant

    $$P_\theta = mrv_\theta + qrA_\theta \sim qrA_\theta \qquad K = \int P_\theta ds \sim q\Phi$$

  - In strong symmetric fields, magnetized particles cannot cross magnetic surfaces

    $$P_\theta = \frac{\partial L}{\partial \dot{\theta}} = mr^2\dot{\theta} + qrA_\theta = const.$$

    $$L = \frac{mv^2}{2} + q\mathbf{v}\cdot\mathbf{A} - q\phi$$

    $$d \le \left| mr\dot{\theta} / qB_p \right|$$

➡ Excellent confinement properties expected for plasmas with arbitrary non-neutrarlity

1. 1999 Yoshida *et al.*, in *NNP Phys. III*.
   2002 Pedersen Boozer, PRL 88, 205002.
   2002 Stoneking *et al.*, PoP 9, 766.

2. 2010 Yoshida *et al.*, PRL 104, 235004.
   2005 Saitoh *et al.*, PRL 92, 255005.

Plasma formation is realized through inward diffusion due to fluctuation-induced asymmetry during beam injection

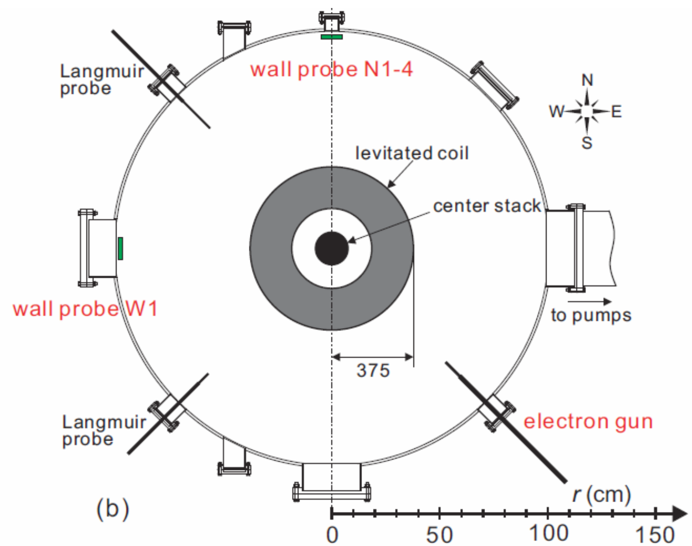

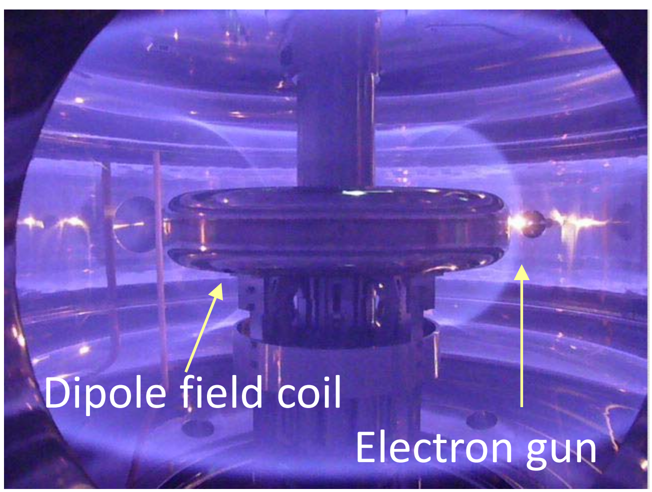

Topview of RT-1 and beam injection

- **Particle penetration into closed surfaces**
  - During beam injection, plasma has fluctuations that induces asymmetry of trap system
    - ➡ Temporal violation of P_θ and K conservations
    - ➡ Effective radial diffusion of particles
  - In RT-1, small electrostatic fluctuations cause effective radial diffusion of particles

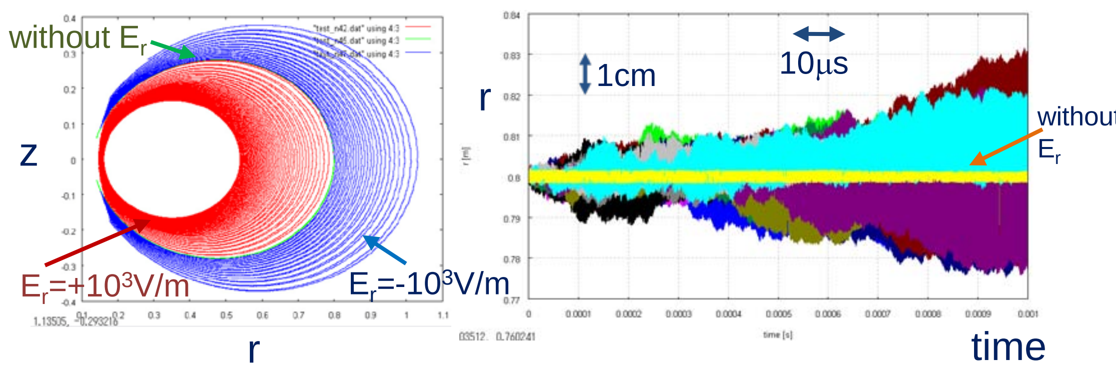

Randum field of 10^3V/m ➡ ~10cm/ms of tansport

- Particles can be transported radially until stable equilibrium state is spontaneously generated

Plasma has large fluctuation during beam injection, and is stably confined after injection ends as fluctuation is stabilized

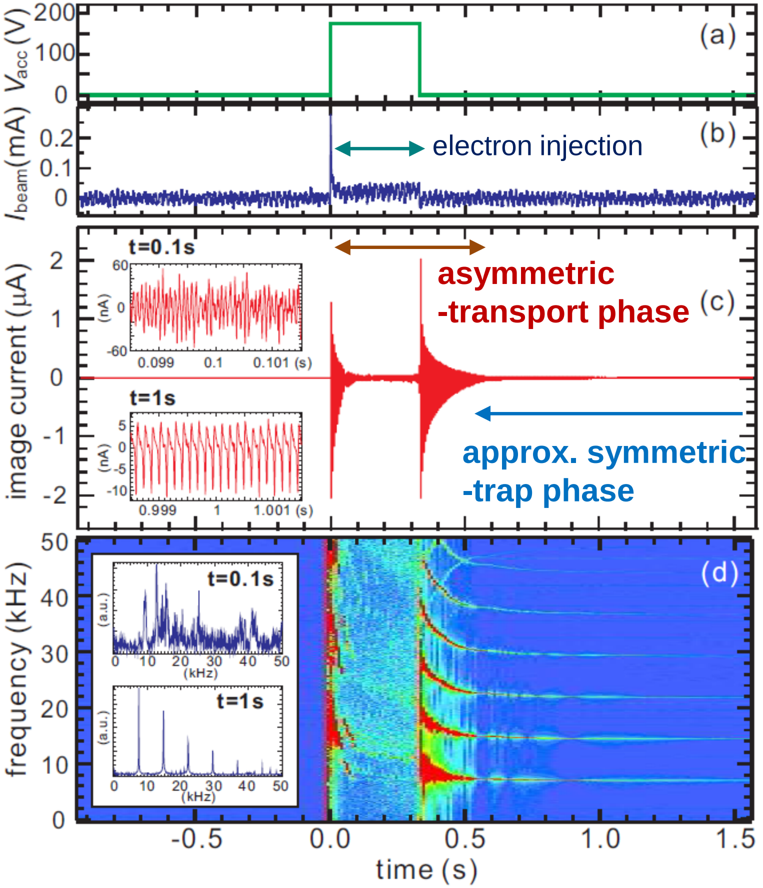

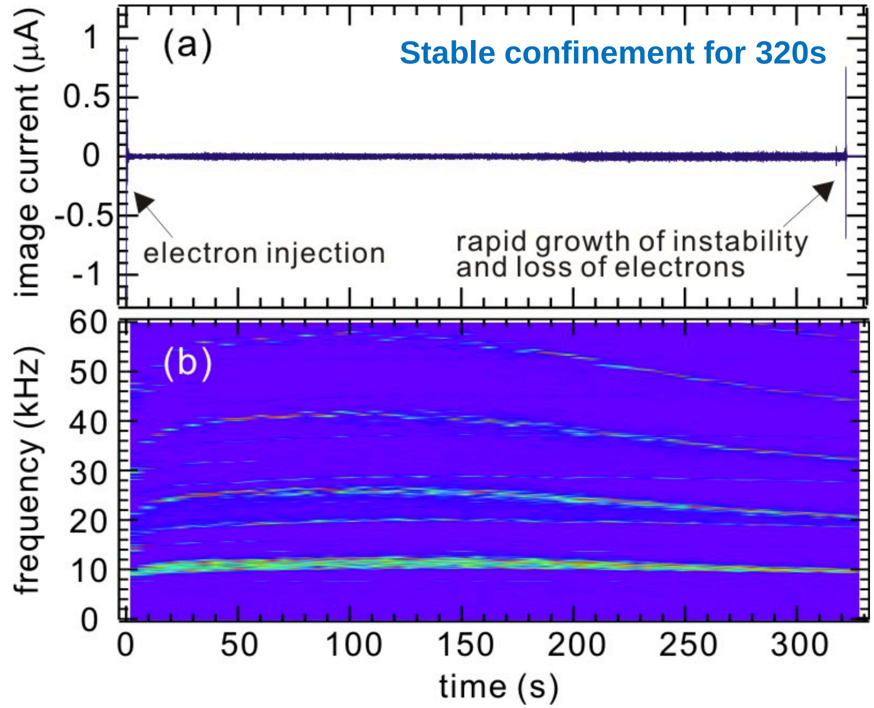

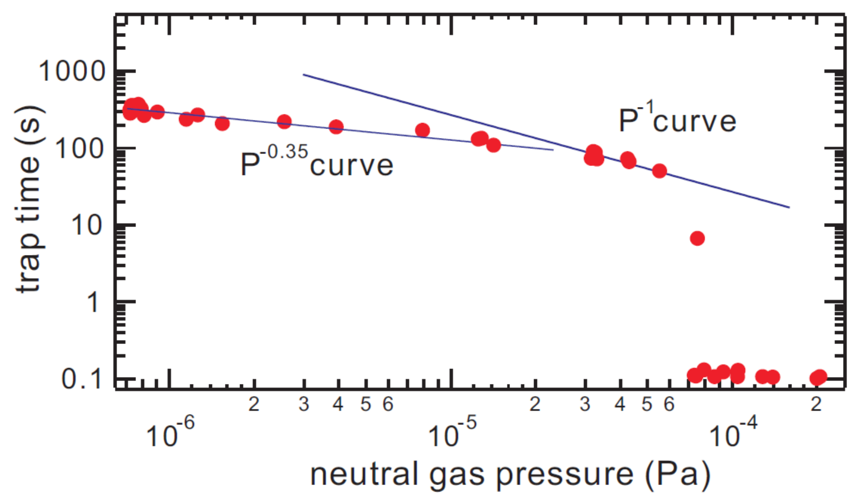

- During injection: turbulent-like fluctuation
- After injection ended: stabilized and trapped for more than 300s (depending on P_n)
- Confinement ends with onset of instability

Spontaneous formation of rigid-rotating equilibrium state 1: Density and potential profiles are consistent with semi rigid motion

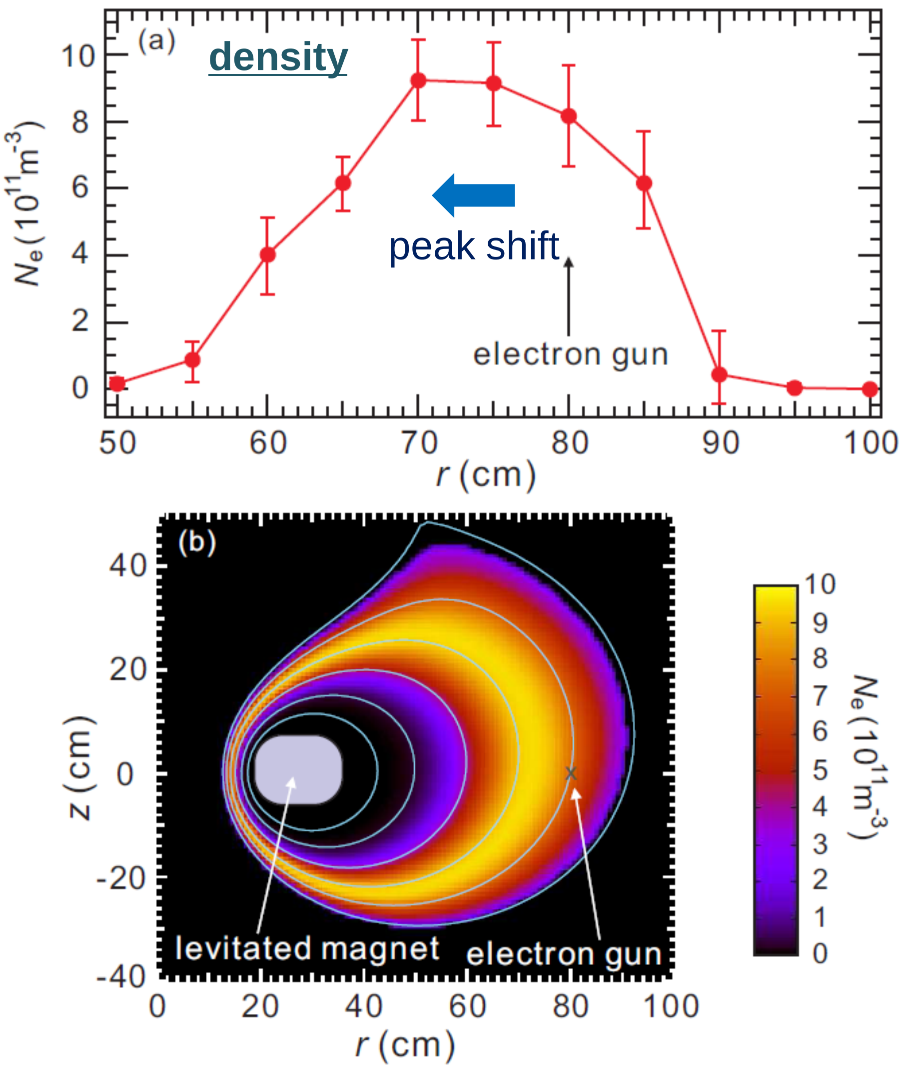

Radial density profile and space potential profiles During beam injection. V_{acc}=500V.

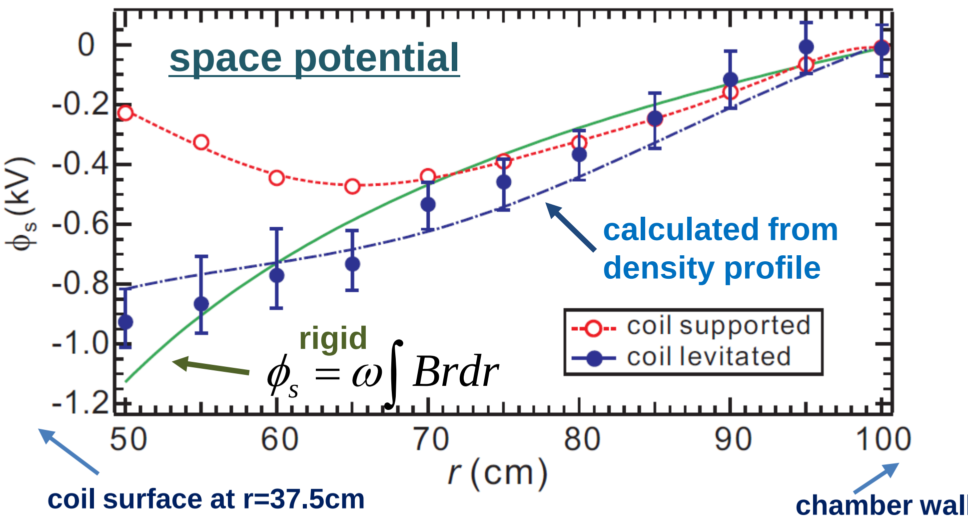

Space potential profiles. V_{acc}=500V.

- Profiles during beam injection are consistent with semi-rigid-rotation
  - Coil levitation results spontaneous charge-up of the coil case

    ➡ flow shear is drastically reduced, and plasma is stabilized
  - Measured and calculated (from density profile) potential profiles are consistent

Spontaneous formation of rigid-rotating equilibrium state 2: Fluctuations indicate toroidal rotation with constant frequency

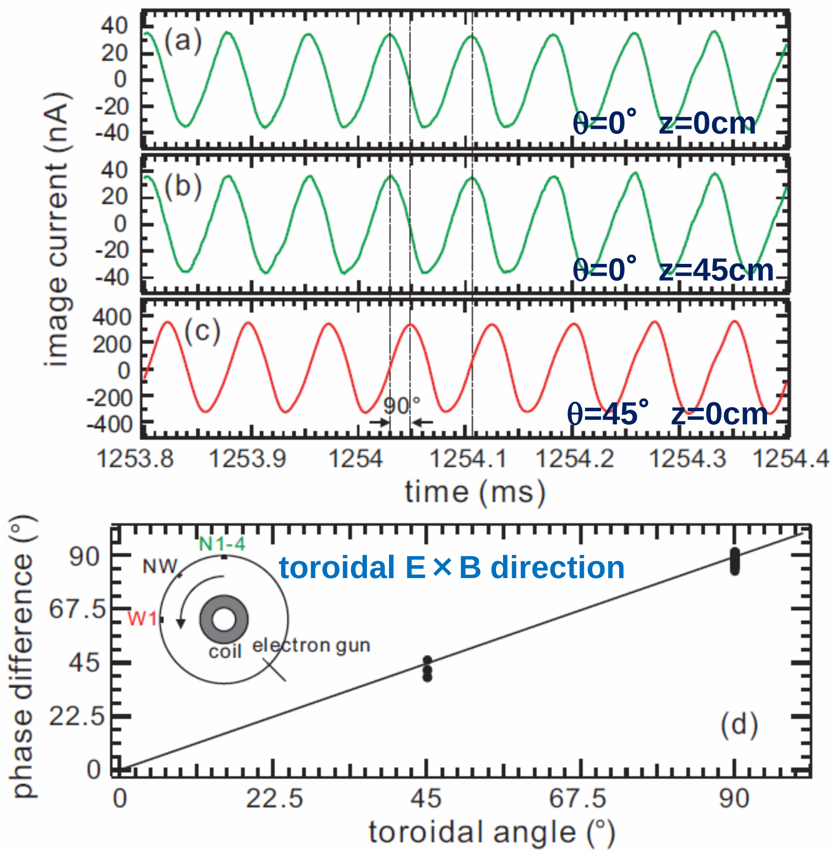

Fluctuations at different θ and z positions

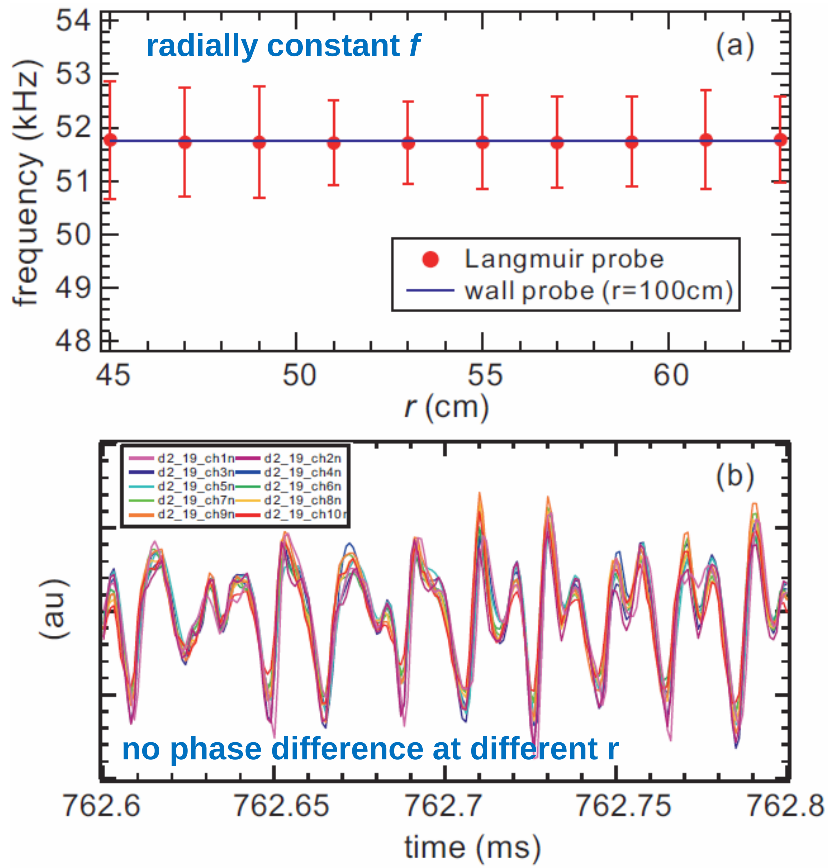

Fluctuations at different radial positions

- Electrostatic fluctuation has phase difference in only toroidal direction (n=1).
- Fluctuation frequency is constant at different radial positions, suggesting rigid-rotating equilibrium of toroidal magnetospheric plasma

Observation of inward particle diffusion 1: Plasma diffuses inward to strong field region

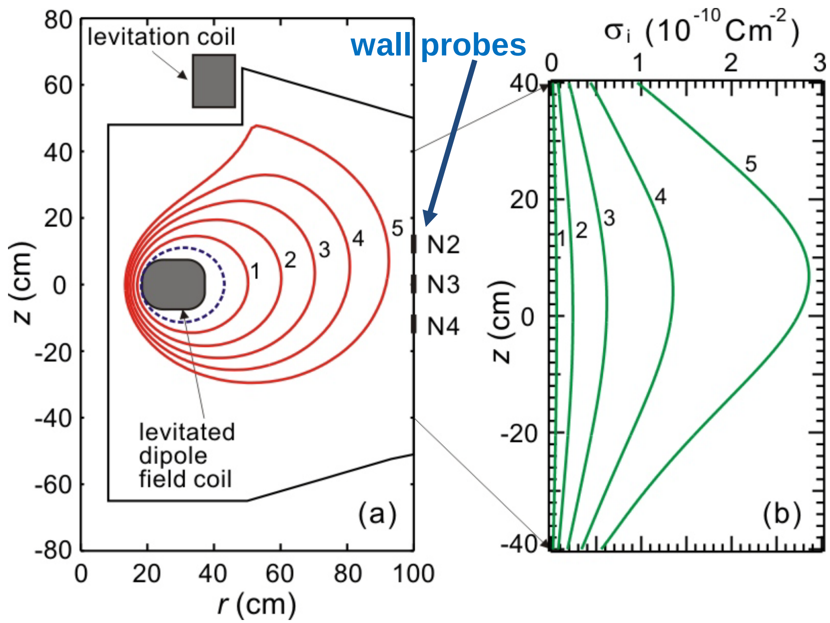

Plasma boundaries and image charge profiles

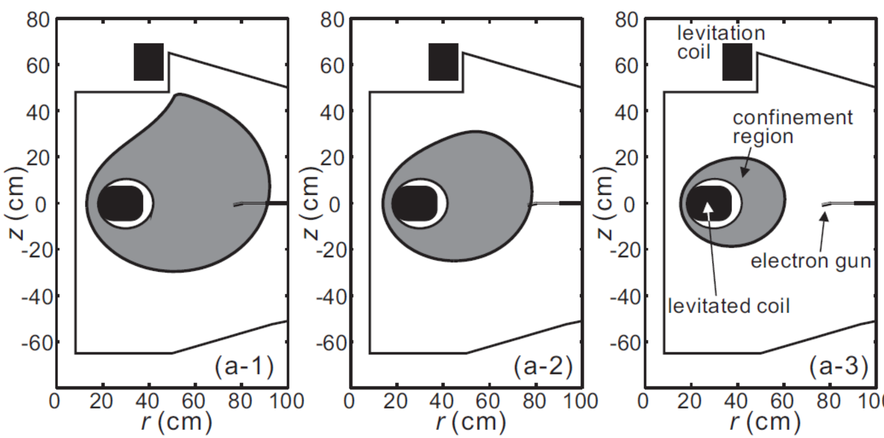

(i) during beam injection ➡ **(ii) just after Injection ends** ➡ **(iii) just before confinement ends**

Ne=1.4×10^{11}m^{-3} < 2.4×10^{11}m^{-3} < 3.2×10^{11}m^{-3}

- Profile measurement by wall probes*1
  - Non-destructive diagnostics is needed for toroidal NNP in closed surfaces
  - Spatial profiles can be estimated using multiple local electric field values

$$E_r = -\int I_i / \varepsilon_0 \, dt$$

- Temporal inward diffusion of particles
  - Profiles measured for three cases:

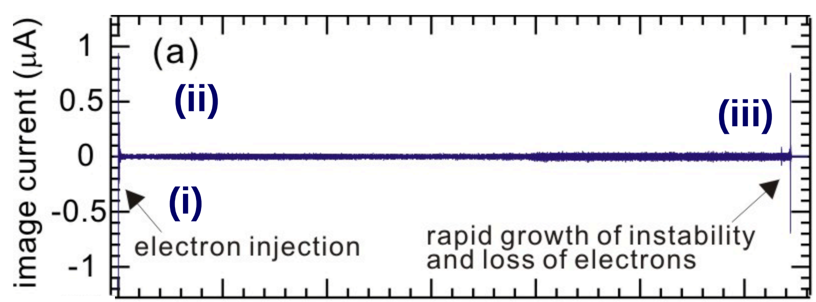

  - Inward diffusion and density increase

1. **2009 Saitoh *et al.*, Plasma Fusion Res. 4, 054**

Observation of inward particle diffusion 2: Space potential exceeds initial electron energy in strong field region

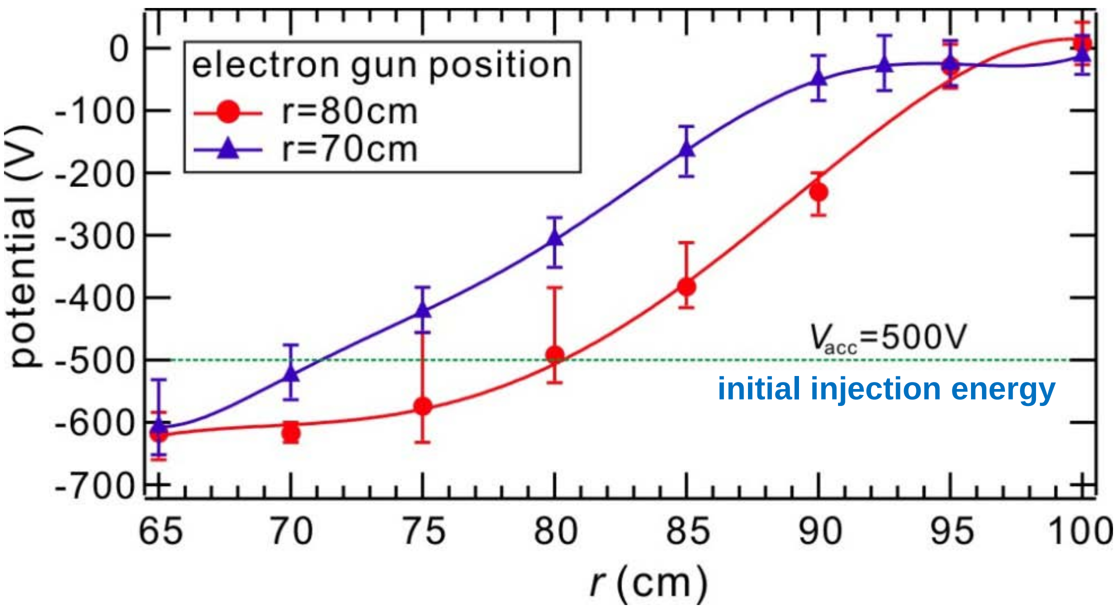

Radial spatial potential profiles with different radial positions of gun. V_{acc}=500V.

- Potential profiles indicate radial transport and acceleration of particles
  - At $r=r_{gun}$, space potential agrees well with V_{acc}
  - Space potential at $r<r_{gun}$ (in the stronger field region) is lower than V_{acc}.

➡ Some particles are accelerated and radially transported inward,
while thermal relaxation time (~400s) is much longer than beam injection time.

Observation of inward particle diffusion 3: Coincident instability onset and radial particle transport

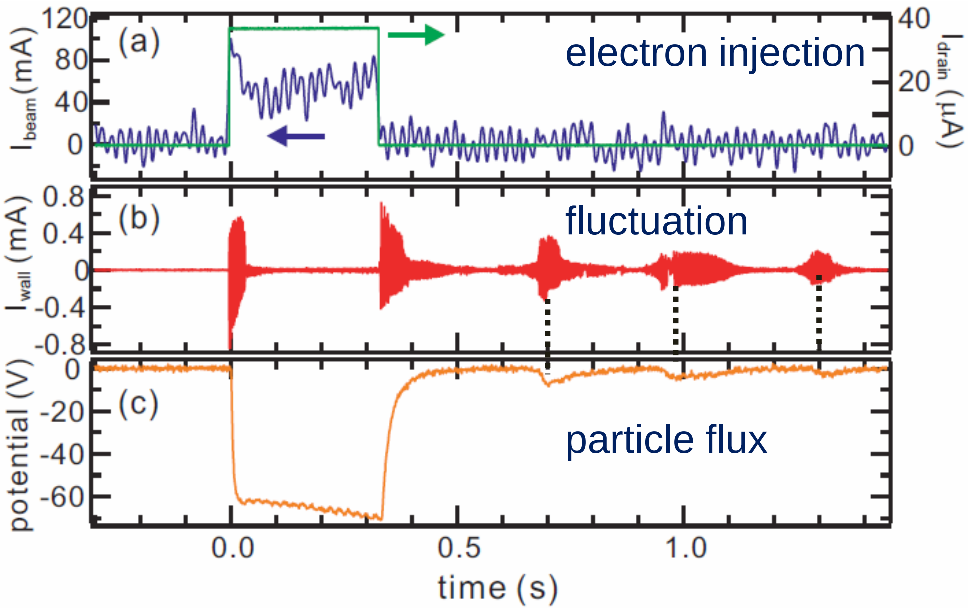

Onset of instability and particle flux at different magnetic surface

- Particle flux measurements show fluctuation-induced radial transport
  - Radial particle transport and onset of instability are simultaneously observed

✓ Fluctuation-induced transport by violation of symmetry and third invariant

✓ Spontaneous generation of rigid-rotating stable vortex

➡ Effective particle injection and confinement of toroial NNP

Section II: High-beta ECH plasma formation

- Stable formation of high-beta plasma: local beta~70%
- Long confinement time of hot electron plasma
- Observation of peaked density profiles in strong field regions

2006 Yoshida *et al.*, Plasma Fusion Res. 1, 006.
2008 Yoshida *et al.*, 22nd IAEA Fusion Energy Conference EX/P5-28.
2009 Yano *et al.*, Plasma Fusion Res. 4, 039.
2010 Saitoh *et al.*, 23rd IAEA Fusion Energy Conference EXC/9-4Rb.

RT-1 has succeeded to produce high beta (local beta~70%) hot electron plasma by ECH up to 45kW of RF injection

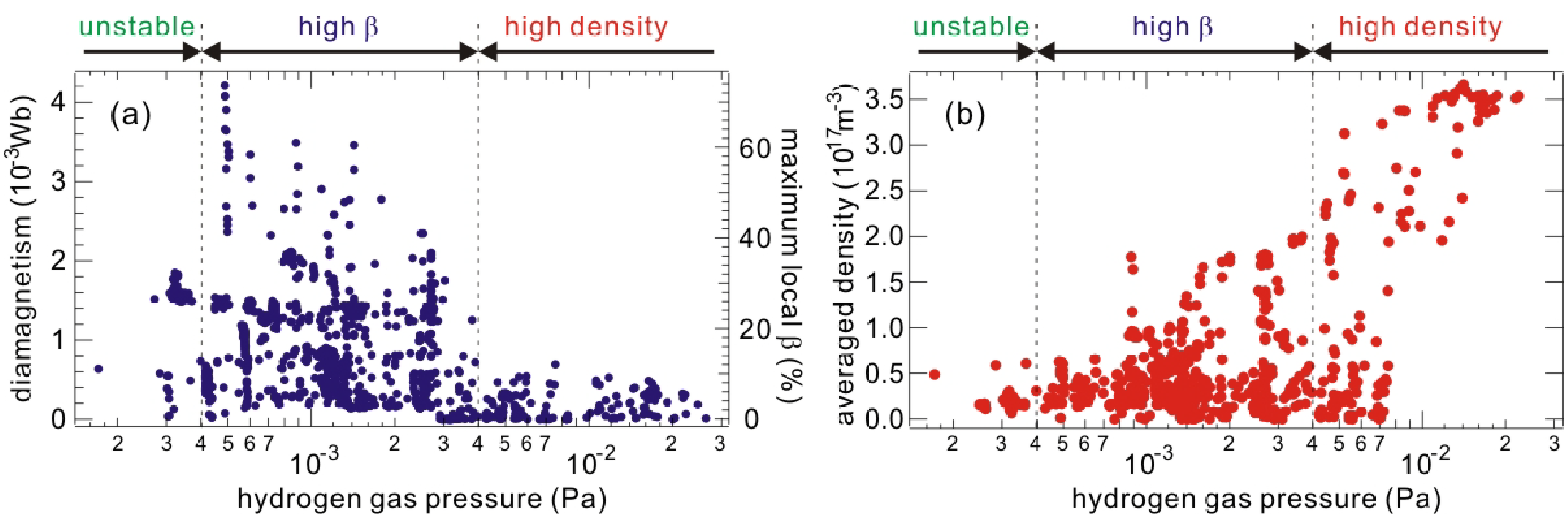

Diamagnetic signal (with calculated maximum local β) and line averaged density

- Optimization of formation conditions and geomagnetic field compensation resulted drastic improvements of plasma properties*[1]

- Parameter ranges designated as high-density, high-β, and unstable states, according to the filling neutral gas pressure

- High-β (density $n_e > n_{cutoff}$) plasma is generated, $\Delta\Phi$=4.0mWb - local β~70% (2d Grad-Shafranov analysis and x-ray measurements are consistent)

1. 2009 Yano *et al.*, Plasma Fusion Res. 4, 039.

High β ECH plasma is generated with optimized formation conditions, avoiding the onset of instabilities

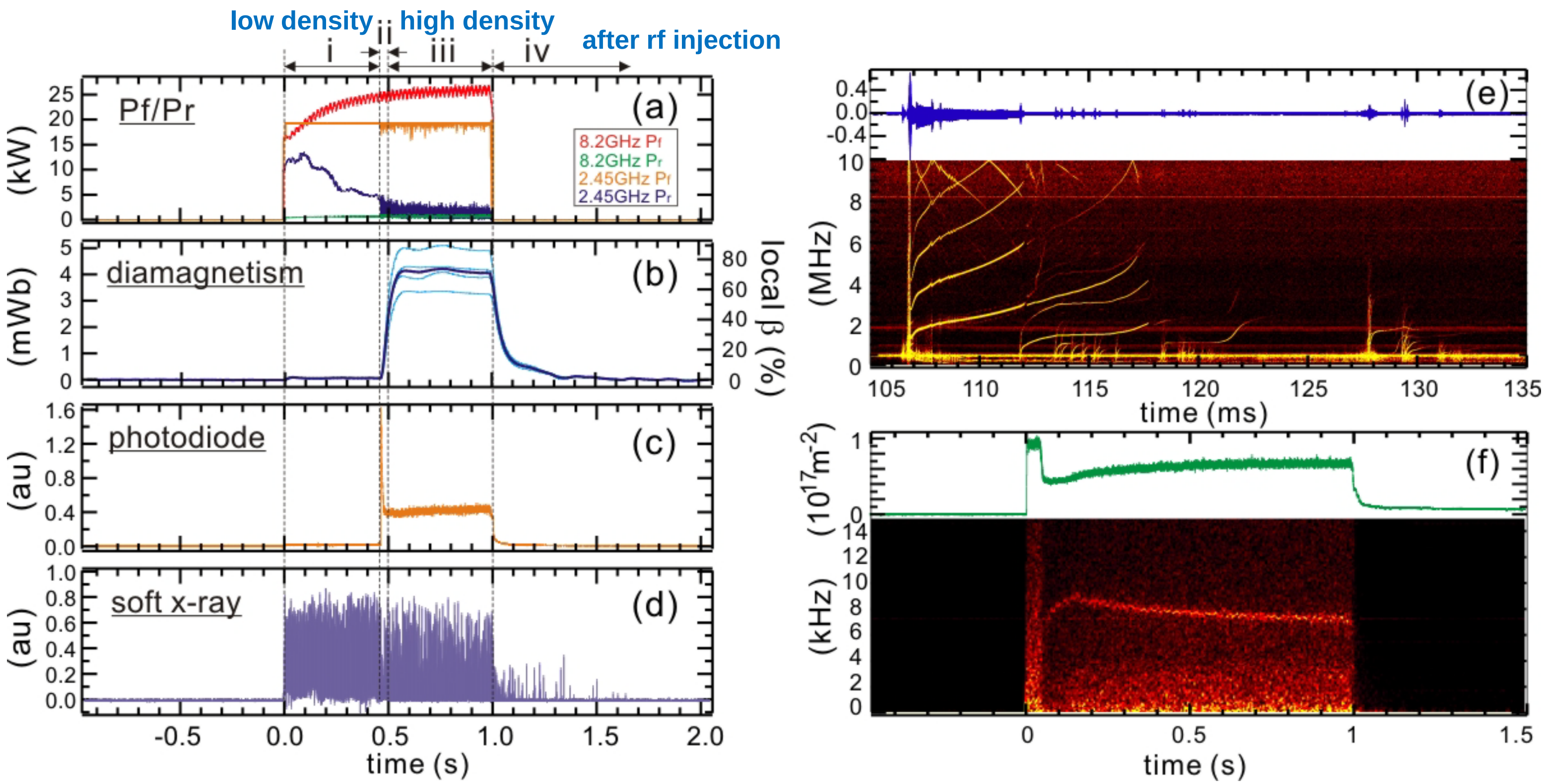

Typical waveforms of high-β plasma and electromagnetic fluctuations in RT-1

- High-β state is characterized by large stored energy, strong x-ray, and depression of visible light strength and fluctuations: **hot electron plasma**

- In phase (i), thin (~$10^{15}m^{-3}$) hot plasma has large electromagnetic fluctuations, which are stabilized after higher density formation in phase (iii)

  - Effects of hot electrons are possible reasons for the onset of instability*[1]

1. 2006 Garnier *et al.*, PoP 13, 056111.

Electrons of high beta plasma consists of majority of hot (up to ~50keV) component, and τ_p~0.5s

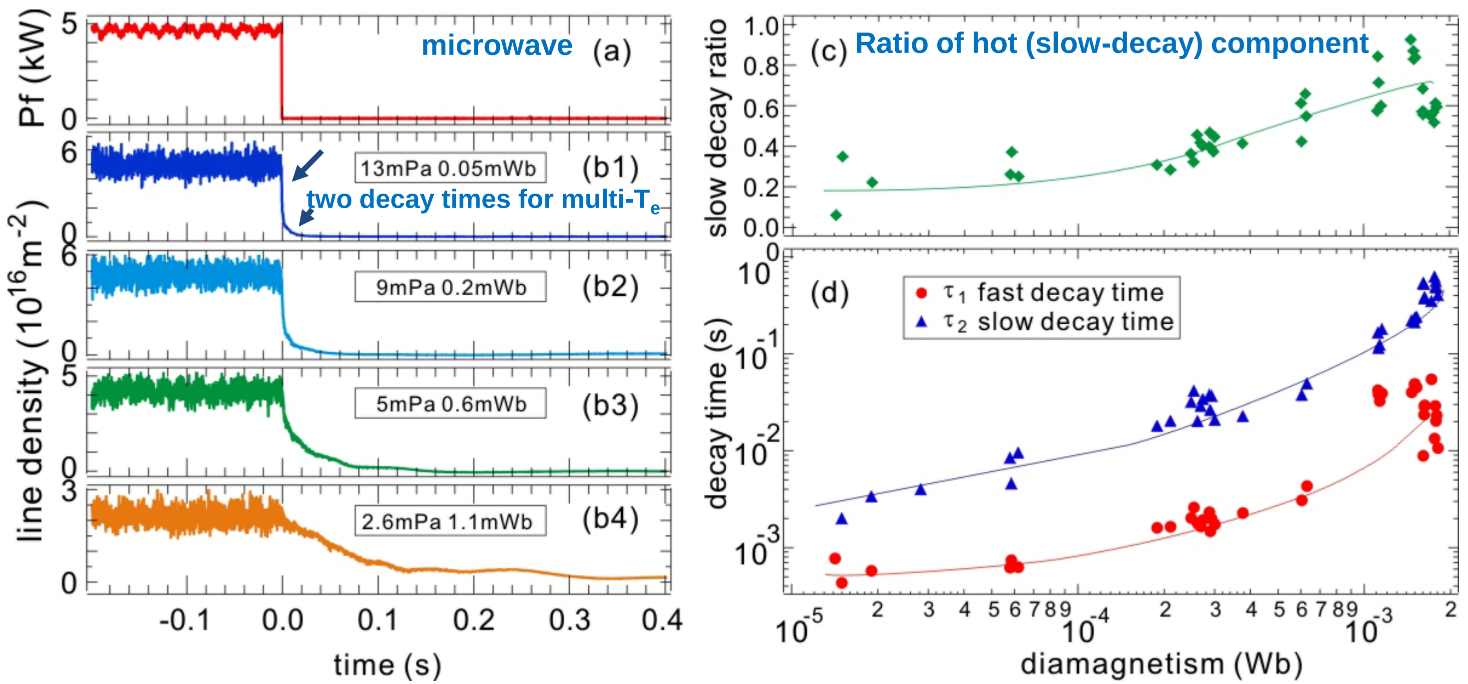

Decay of line density and estimated ratio of hot-electron component and confinement time

- Electrons consists of majority (~60%) of hot (~50keV) and cold (~10eV) populations
- Confinement time of hot electron component is τ_p=0.5s cf) τ_{Bohm}~1.4μs
- Energy confinement time τ_E is comparable to τ_p, suggesting that temporal variation of T_e is relatively small after RF stopped (consistent with x-ray measurements)

Plasma has peaked density profiles in strong field region when superconducting magnet is levitated

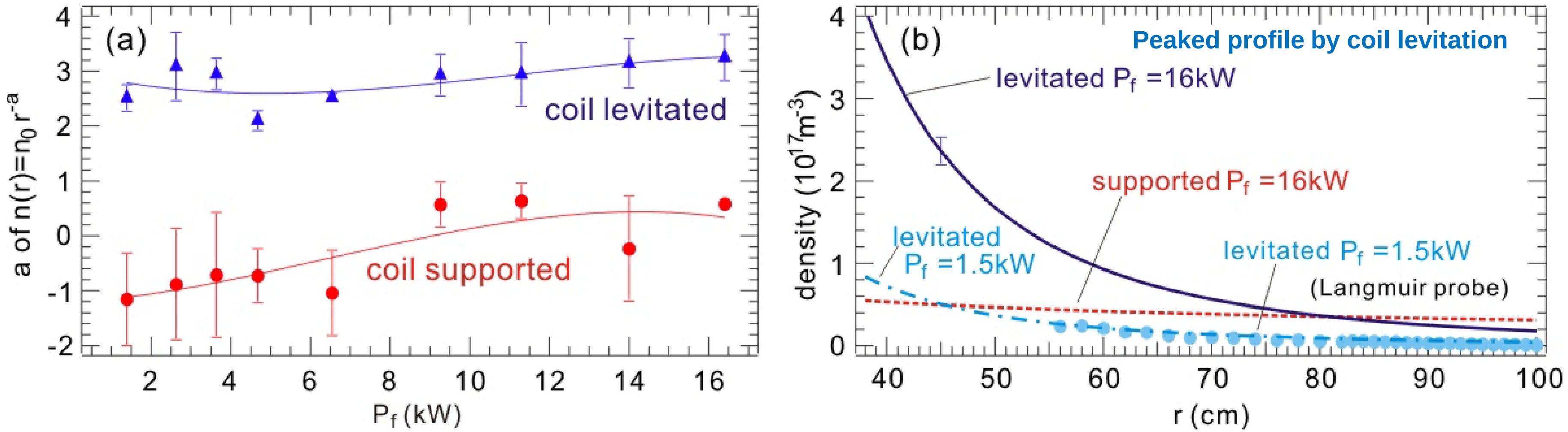

Radial density profiles [coefficient *a* of $n(r)=n_0 r^{-a}$] with and without coil levitation

- Density profiles were estimated by multi-cord measurements of interferometer, assuming $n(r)=n_0 r^{-a}$ on z=0 plane and density is a function of magnetic surface
- When the superconducting coil is levitated, plasma has peaked density profiles
- This result is similar to previous report in LDX*[1] and consistent with Hasegawa's prediction*[2] that turbulent-induced diffusion occurs until plasma density per flux tube becomes constant: $\partial/\partial\psi \iint f(\mu, J, \psi) d\mu dJ = 0$

1. 2010 Boxer *et al.*, Nature Phys. 6, 207. 2. 1987 Hasegawa, CPPCF 11, 147.

Summary: RT-1 experiment 2006-2010

- **High-β ECH plasma** *Yano et al*., Wednesday Morning Poster NP9.39
  - **local β=70%**, hot component is majority of electron populations, τ_p= **0.5s**
  - Plasma has **peaked density profiles** as predicted by Hasegawa
  - High-β state is realized by suppressing **electromagnetic fluctuations**

- **Toroidal magnetospheric non-neutral plasma**
  - **Pure electron plasma trapped for 320s**, comparable to classical diffusion time
  - Spatial structures and fluctuation properties suggest **self-organization of toroidal rigid-rotating equilibrium** state
  - **Inward diffusion** and density increase in strong field region were non-destructively observed

Future tasks

- High-β plasma: **ion heating**, **investigation of Hall effects**, **β limit**
- NNP: applications for trapping **antimatter plasmas** (e^+, e^+-e^-)

Backup Material

including preliminary data

Soft x-ray imaging of hot electron plasma

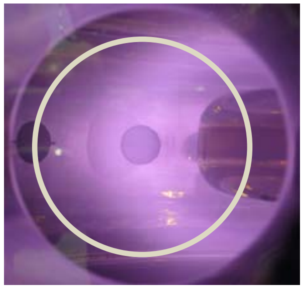

Visible light image from port 1 and image area of x-ray CCD camera.

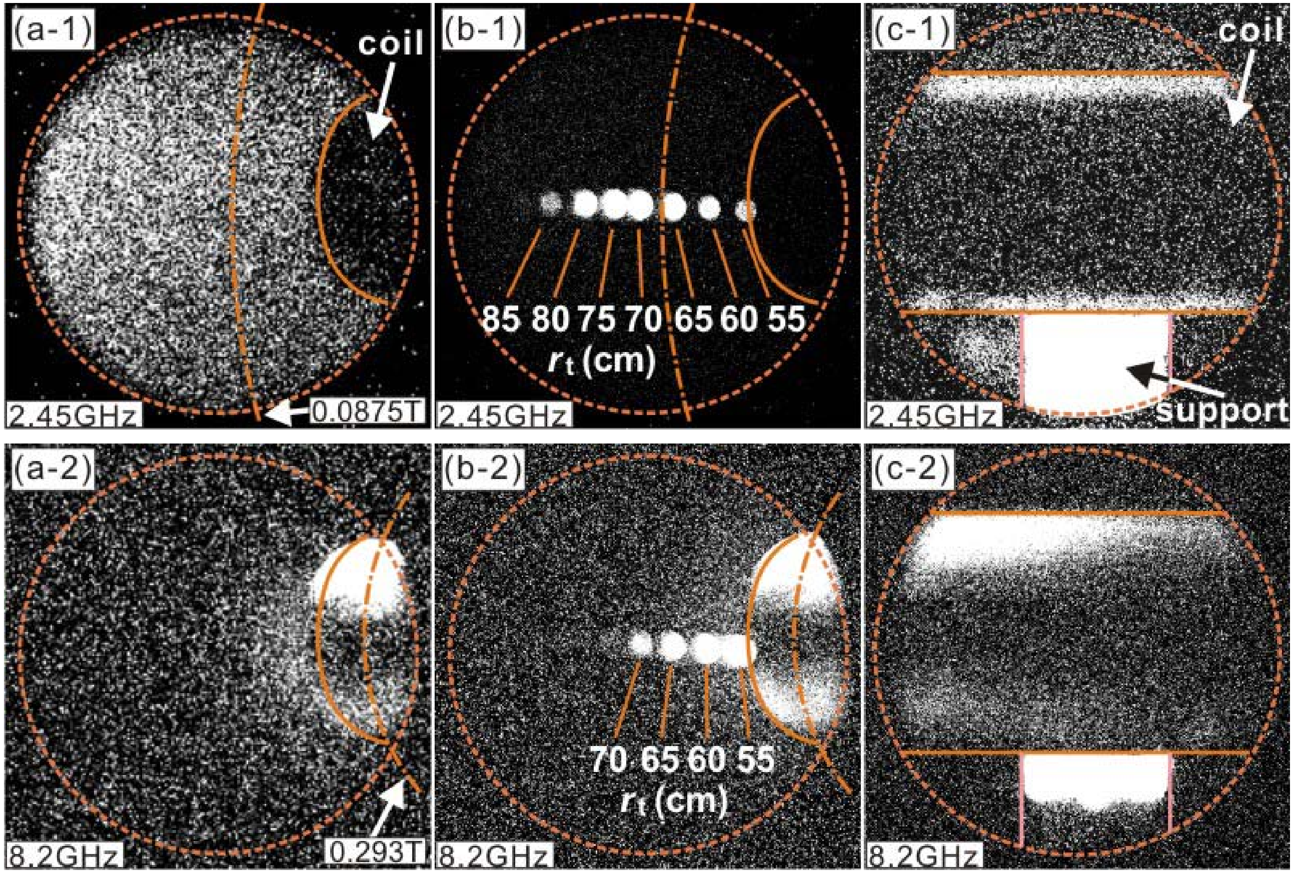

Soft x-ray images observed from (a) port 1, (b) port 1 with insertion of target tube At different radial positions, and (c) port2. (1) 2.45GHz and (b) 8.2GHz ECH.

- 2.45GHz: hot electrons fill approximately entire region in the image circle
  8.2GHz: x-ray emitting region localized near the coil, some lost on coil surface
  - Relatively large diamagnetic signal observed for 2.45GHz rather than 8.2GHz.
- Coil support structure is the main loss channel of hot electrons without levitation.

High beta plasma with optimized neutral gas pressure

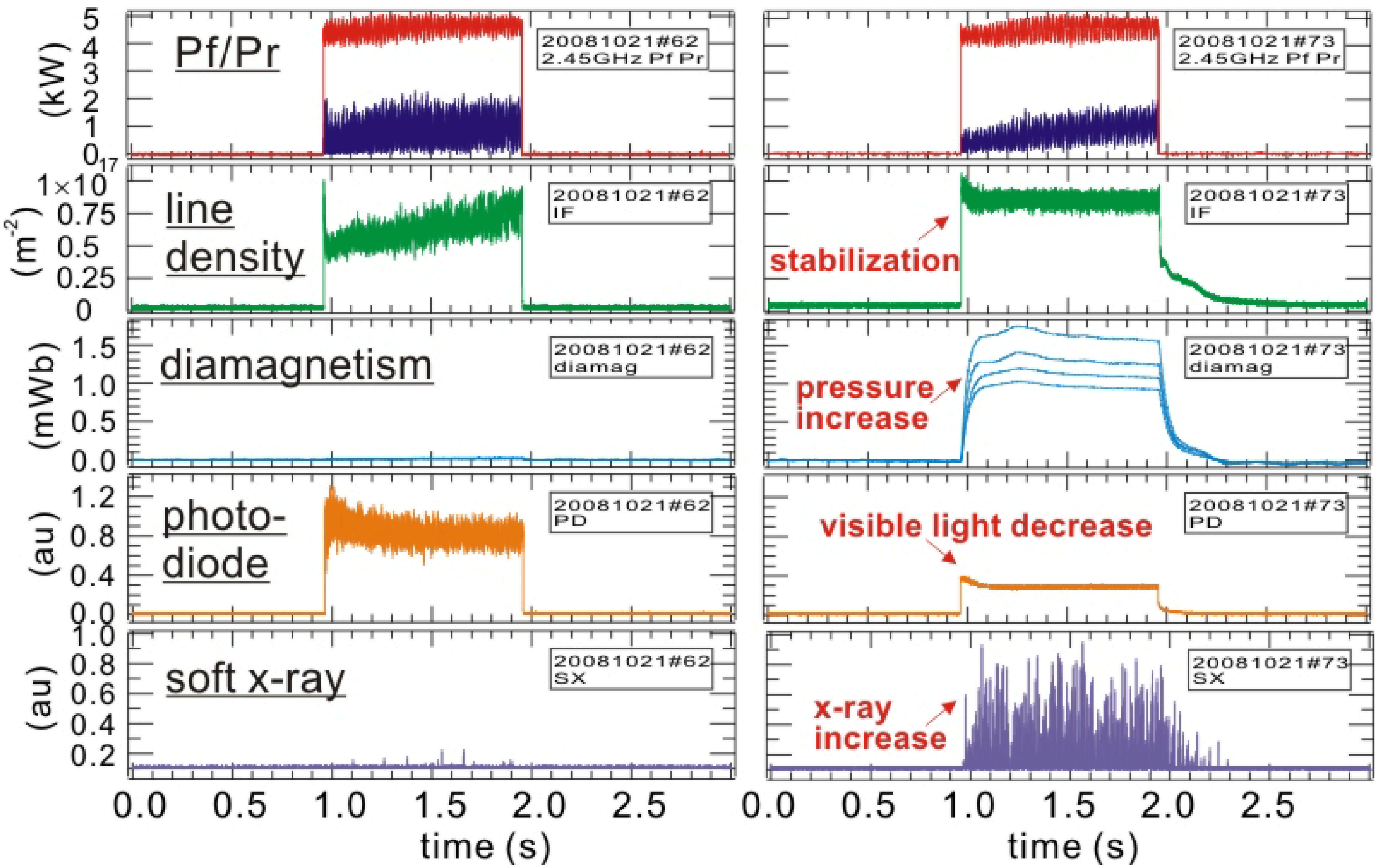

Waveforms of ECH plasma in RT-1 with (a) P_{H2}=4.5×10^{-2}Pa (b) 1.3×10^{-3}Pa.

- By optimizing neutral gas pressure, high-β plasma is generated.
- Plasma pressure is mainly resulted from hot component of electrons (~50keV).

High-β discharge and stabilization of fluctuation

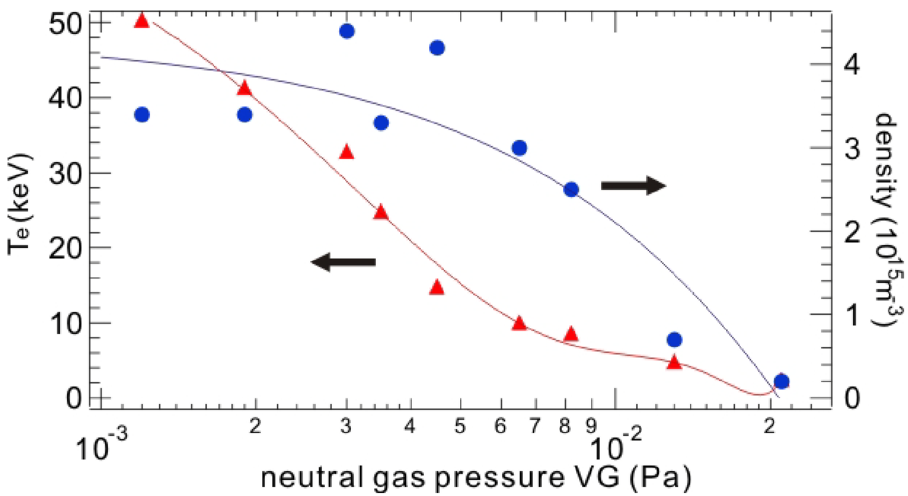

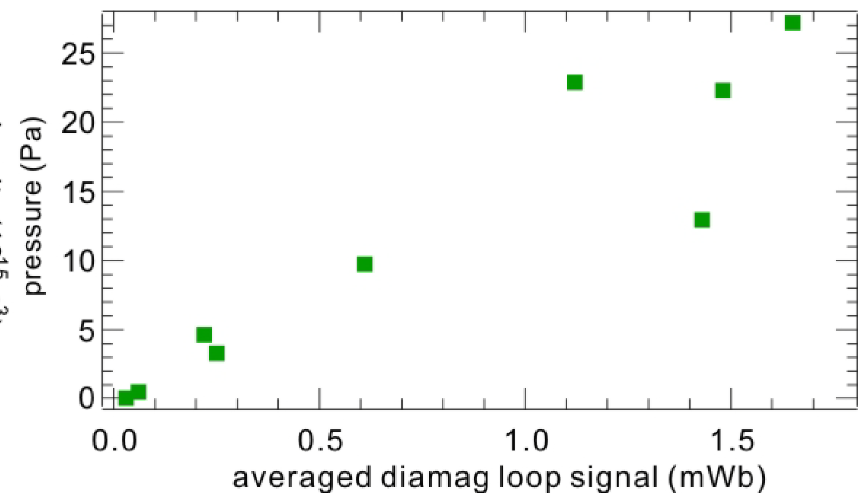

Temperature and density of hot electrons in variation of filled neutral gas, and hot electron pressure $P_h = n_h T_h$ in variation of diamagnetic signal.

- High-β Plasma pressure is mainly resulted from hot electrons.
- Plasma has hot component electrons of T_h~50keV.
- Strong correlation between $P_h = n_h T_h$ and diamagnetism suggests hot component is the main component of electrons in high-β cases.

Hot electron imaging by x-ray CCD camera

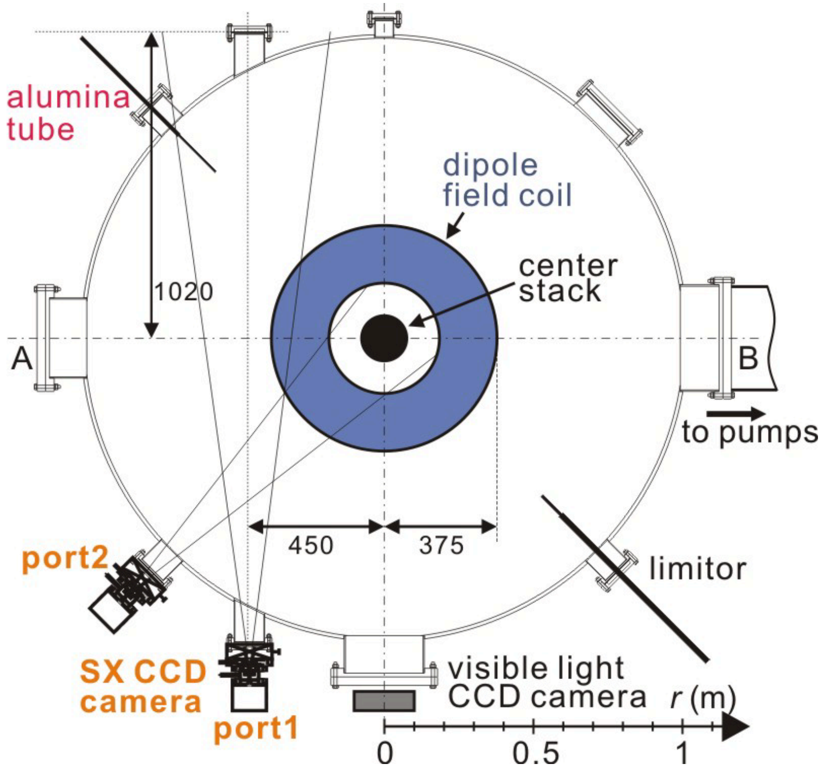

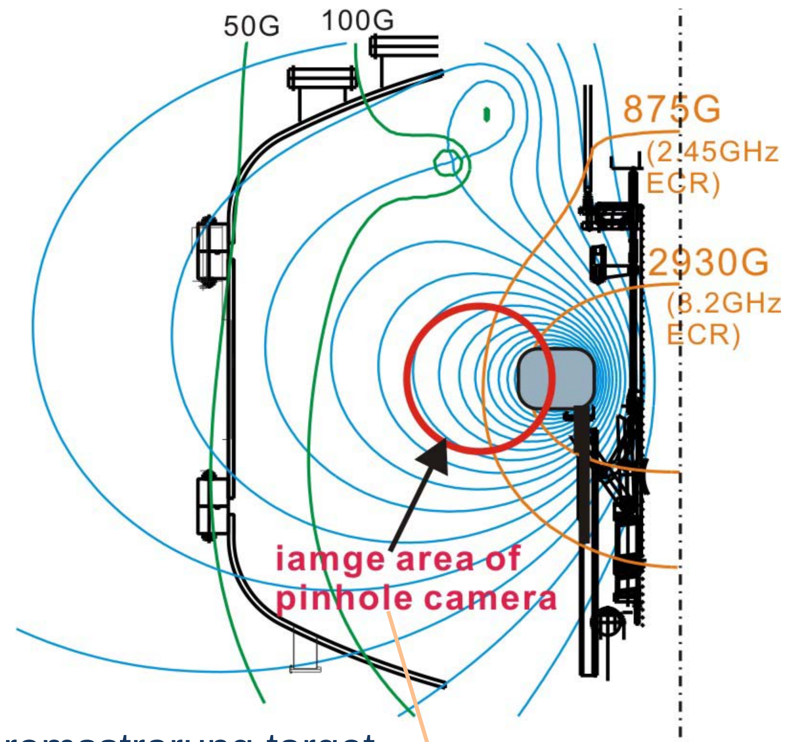

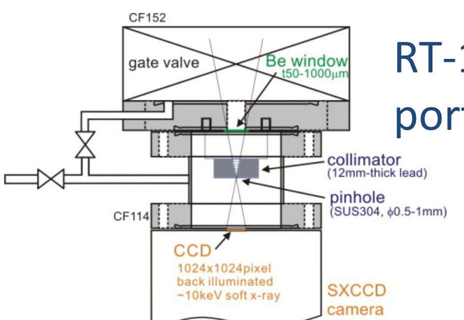

RT-1 cross section, camera ports, and camera construction.

Bremsstrarung target (ceramic tube)

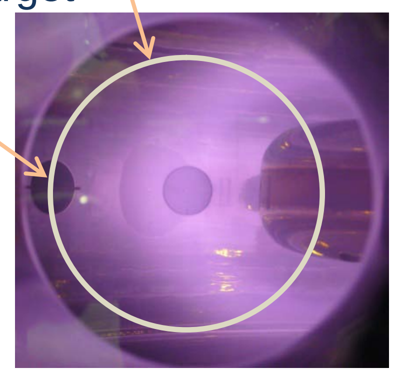

Visible light image from port 1

Visible light view from port1

➢Soft x-ray CCD camera

·1024×1024 pixel (13×13mm), 16bit dynamic range

·Be window (100um), collimator, tantalum pinhole

Soft x-ray (photon counting mode of CCD camera)

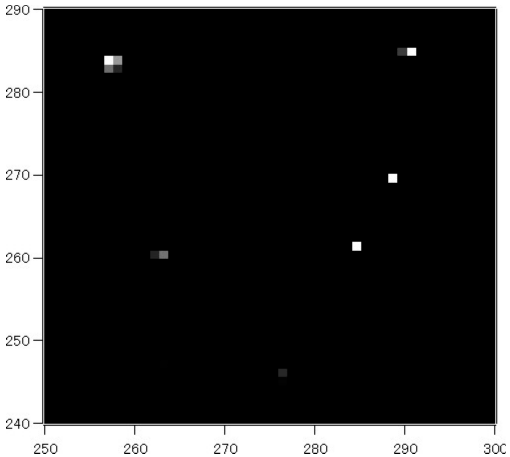

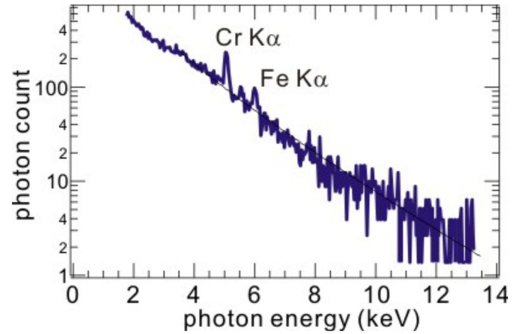

Enlarged CCD image and pulse height analysis

- ➢Pulse height analysis of photon energies with CCD
- ➢Impurity lines are used for energy calibration
- ➢T_e is approximately constant in the image circle…
- ➢Experiment with coil levitation is future task

Preliminary results without coil levitation

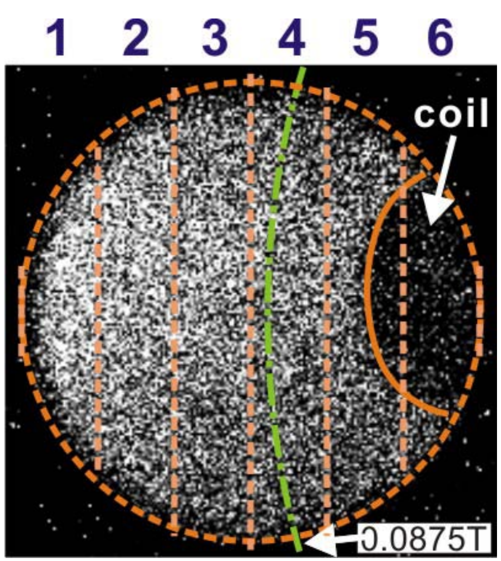

Separated image region and photon energy spectrum

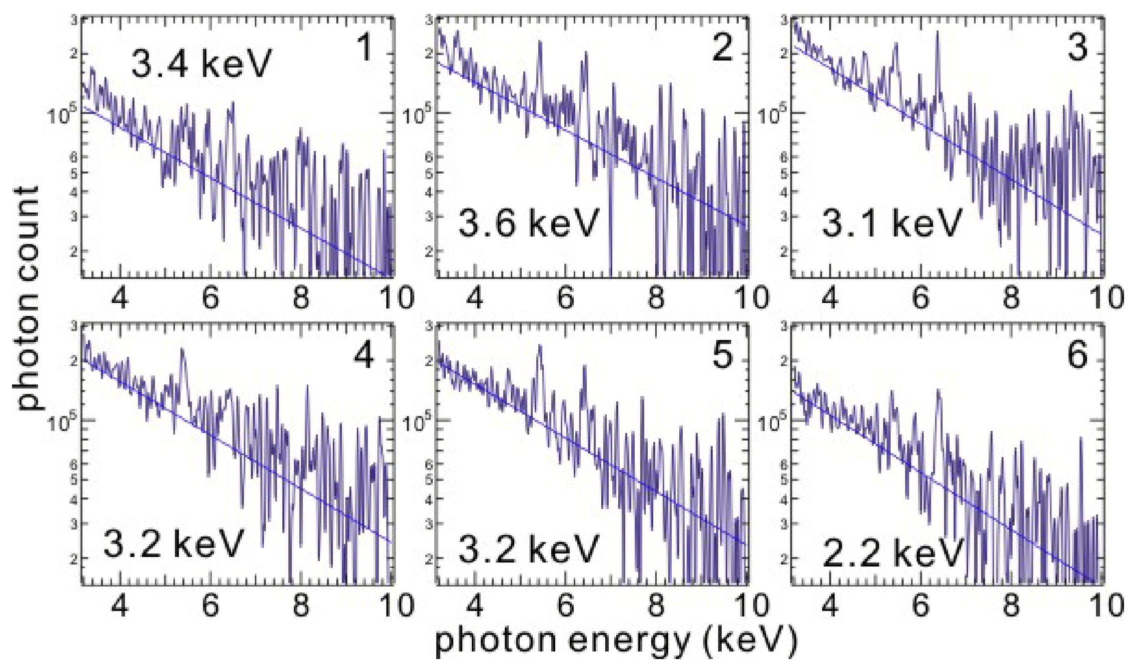

* Y. Liang *et. al.*, Rev. Sci. Instrum. **72**, 717 (2001), H. Saitoh *et. al.*, PFR **4**, 050 (2009).

Grad-Shafranov equilibrium analysis

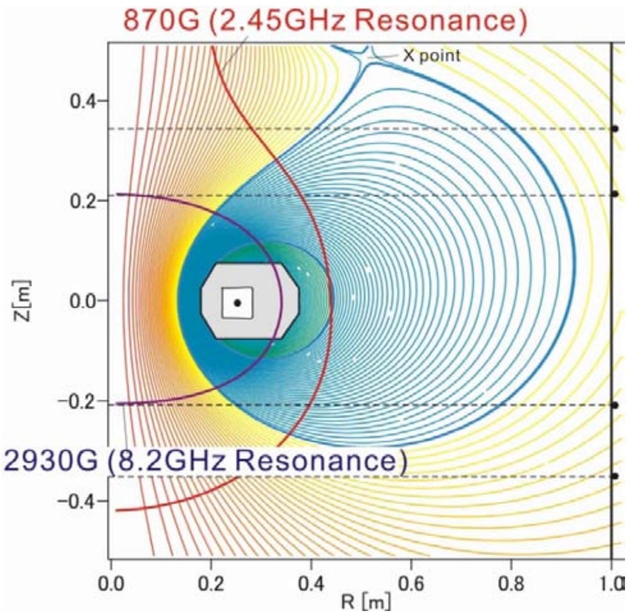

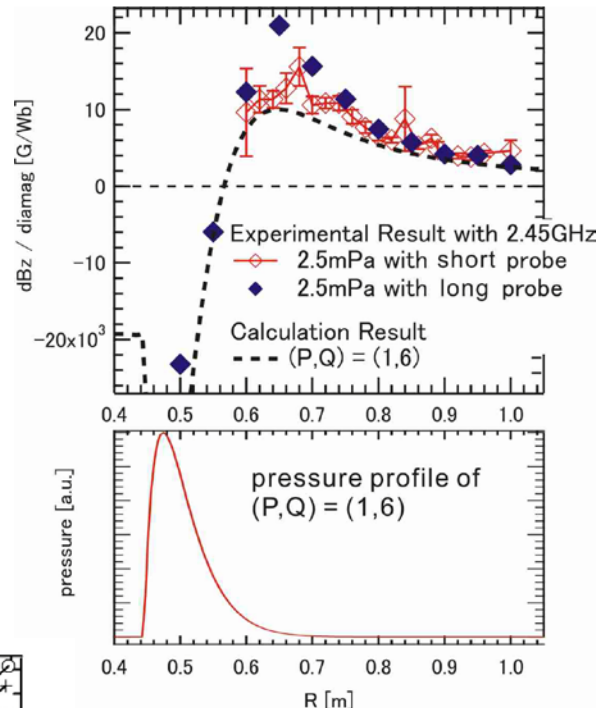

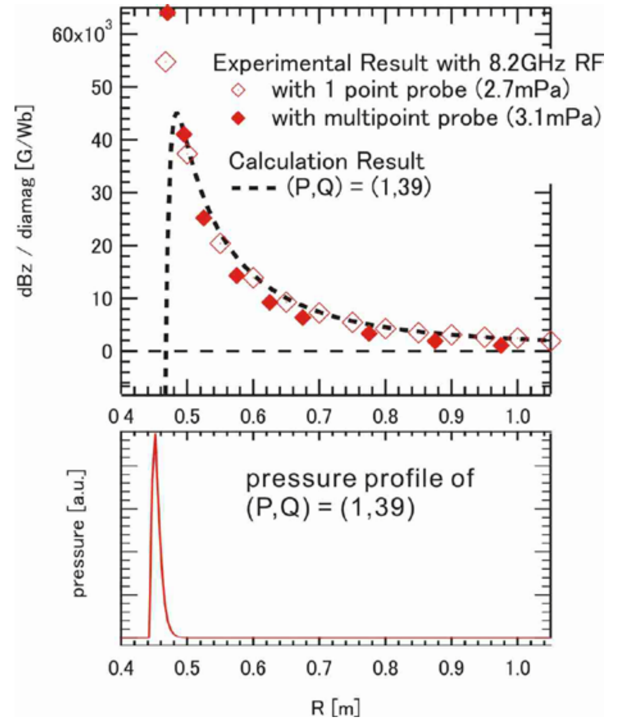

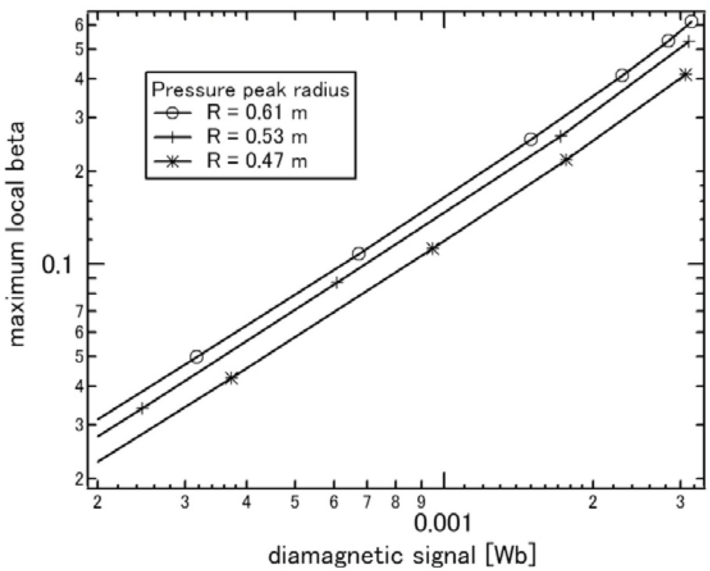

- Diamag loop signal and local β values
- Pressure profiles have steep gradient near the superconducting coil.

Energy confinement time and β values

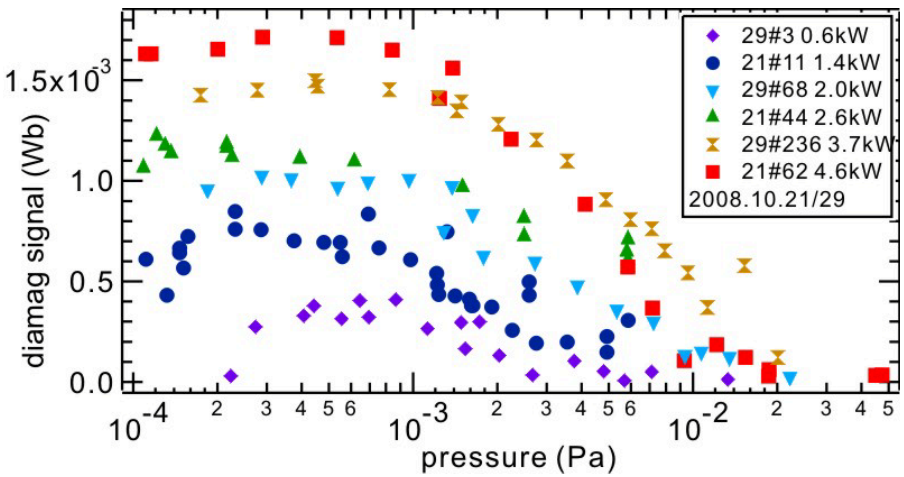

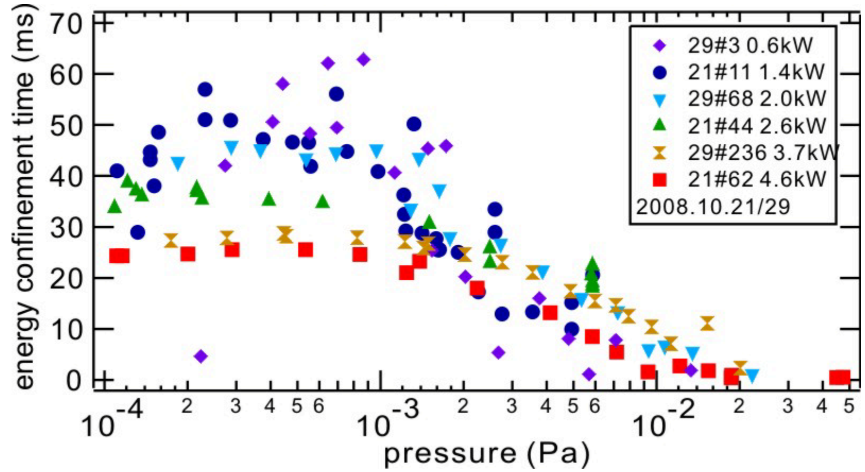

Plasma pressure (diamagnetic signal) and energy confinement time

- Hot electron population reaches ~30% by reducing neutral gas pressure.

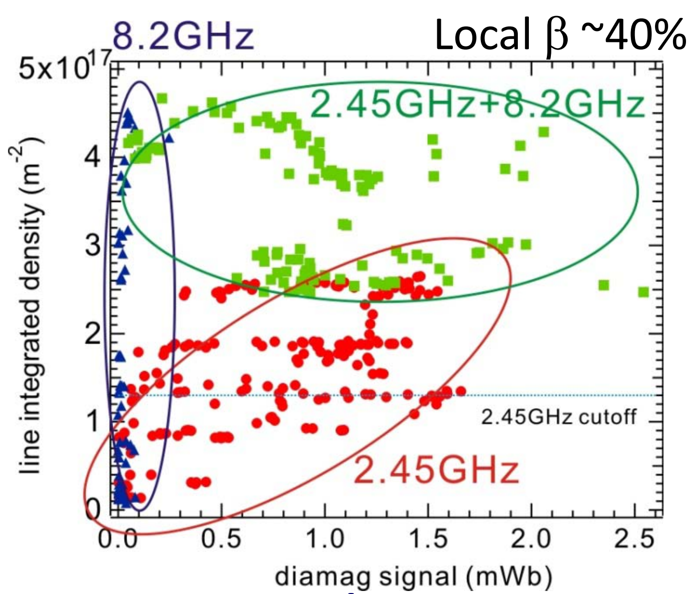

Diamag-Ne, 8.2/2.45GHz ECH

- Energy confinement time estimated from from stored energy and injected RF power is τ_{e1}~60ms.
- τ_{e1} is shorter than that estimated from magnetic measurement (diamag-decay time) of τ_{e2}~500ms.
- The stored energy is typically higher for 2.45GHz ECH